



# NASA Public Access

Author manuscript

*Int Conf Environ Syst.* Author manuscript; available in PMC 2020 June 22.

Published in final edited form as:

*Int Conf Environ Syst.* 2019 July 07; 49: .

## Design and Control of Reduced Power Actuation for Active-Contracting Orthostatic Intolerance Garments

**Rachael M. Granberry,**

University of Minnesota, Department of Design, Housing, and Apparel, Saint Paul, MN, 55108

**Santo Padula II,**

NASA Glenn Research Center, Cleveland, OH, 44135

**Kevin Eschen,**

University of Minnesota, Department of Mechanical Engineering, Minneapolis, MN, 55455

**Julianna Abel,**

University of Minnesota, Department of Mechanical Engineering, Minneapolis, MN, 55455

**Brad Holschuh**

University of Minnesota, Department of Design, Housing, and Apparel, Saint Paul, MN, 55108

### Abstract

Active-contracting fabrics are an emerging innovation that could revolutionize aerospace compression garment technology, notably orthostatic intolerance garments (OIG), by contracting on demand. Prior research has found that active-contracting fabrics, specifically weft knit garter fabric architectures constructed with shape memory alloy (SMA) filaments, can apply 2-54 mmHg on the body (single-layer construction) or 4-104 mmHg (double layer construction), depending on body radius. Prior garment prototyping and performance validation efforts have been conducted with commercially available Flexinol® wire with an actuation finish temperature of 90°C, a temperature that is not appropriate proximal to the human body. While other chemistries of SMA having lower actuation temperatures used for medical devices inside the human body ( $T_{\text{core}} \approx 37^\circ\text{C}$ ) are commonly available, SMA has not been optimized for actuation control against the human skin ( $T_S \approx 31^\circ\text{C}$ ). This research characterizes and validates a novel SMA material designed by Fort Wayne Metals specifically for actuation adjacent to the surface of the body. Through experimental temperature-force-displacement testing on both Dynalloy Flexinol® and Fort Wayne Metals straight SMA wire and SMA knitted actuator configurations, we present data that suggests (1) performance differences between low-temperature, nickel-rich SMA (Fort Wayne Metals) and high-temperature, titanium-rich SMA (Dynalloy Flexinol®) are negated by certain SMA knitted actuator structures, and (2) certain SMA knitted actuator configurations increase in force upon cool down, offering new concepts for SMA system actuation/control that minimize power consumption and waste heat. This manuscript presents experimental evidence for a future OIG that is donned in an oversized and compliant state, heated momentarily above ambient skin temperature to initiate actuation, and remain fully ‘activated’ once the actuation is complete upon equilibration with skin temperature. The result is an OIG that requires low-operating power that could be doffed through zipper releases and placed in a sub-zero chamber to return the structure to the ‘off’ state for reuse.

## I. Introduction

AEROSPACE compression garments, such as space suits, vertical loading garments, orthostatic intolerance garments, and anti-g suits, require dynamic control of on-body pressure. Recent research on smart material actuators present an alternative technology to traditional pneumatic actuation, suggesting a promising future for aerospace garments<sup>1,2</sup> Examples of smart materials actuators include shape memory alloys (SMA), shape memory polymers, or carbon nanotubes configured in spring, braid, knit, or weave structures.<sup>3</sup> While smart materials, specifically SMA, have been found to meet the force requirements of orthostatic intolerance garment (0.8-7.3 kPa) and even mechanical counter pressure suits (29.6 kPa),<sup>1,2</sup> actuation control has only been demonstrated with commercially available materials that require both (1) high operating temperatures ( $T > 60^{\circ}\text{C}$ ) and (2) a continuous heat source, generally a battery supply. These high operating temperatures pose burn risks to the body and the body insulation required to mitigate this risk adds significant system bulk.<sup>4,5</sup> Additionally, continuous battery supplies are impractical for most aerospace garments that must function in environments with both limited space and power. Parallel research has explored leveraging body heat as the power source for SMA materials having lower transition temperatures. While initial research has found actuator control challenging due to the small temperature threshold between approximate ambient temperatures ( $T_{\text{amb}} \approx 25^{\circ}\text{C}$ ) and approximate skin temperatures ( $T_{\text{S}} \approx 31^{\circ}\text{C}$ ), further investigation and material refinement is warranted.<sup>6</sup>

In an attempt to improve upon prior investigations of body heat controlled SMA actuation, this research characterizes a new smart material and structure combination designed specifically for shape memory control on the surface of the skin. Rather than relying solely on skin temperature or battery supply to drive up and maintain heat for SMA actuation, a smart material and structure pairing was designed to actuate completely at lower temperatures ( $T = 41^{\circ}\text{C}$ ) and increase in force upon cool down, hitting maximum forces at approximate skin temperature ( $T_{\text{S}} \approx 31^{\circ}\text{C}$ ). The implication of this control strategy is a system that requires only initial heating (power) and remains fully stiffened upon cooling to skin temperature ( $T_{\text{S}} \approx 31^{\circ}\text{C}$ ), consuming only a fraction of the power (and generating none of the wasted heat) of prior SMA system designs. To evaluate the feasibility of the proposed reduced-power control strategy, this study characterized the behavior of the novel SMA material and structure combination to determine their appropriateness for future use.

### A. Shape Memory Alloy (SMA) Knitted Actuators

Shape memory alloys (SMAs) are one class of smart materials and are characterized by thermomechanical or magnetomechanical coupling. Nickel titanium alloys (NiTi) are a common type of SMA that exhibit high recovery strains (~6-8%) and high recovery stresses (500-900 MPa) in response to changes in temperature, making them excellent thermomechanical actuators.<sup>7</sup> This characteristic phase transformation is enabled by the transition from a high-temperature, ordered-cubic austenite phase to a low-temperature, monoclinic martensite phase.<sup>8</sup> Fully martensitic NiTi can be deformed under low forces such that twinned (stress-free) martensite variants are deformed into detwinned (stressed) martensite variants.<sup>8</sup> Unlike other metals, SMAs can return to their original structural shape

post-deformation upon heating above the material-specific austenite finish temperature ( $A_f$ ).<sup>7</sup> This structural recovery due to oscillation between cubic and monoclinic structures is referred to as the shape memory effect.<sup>7</sup> The shape memory effect characteristic of SMA makes the material ideal for use as an actuator for dynamic systems applications. Additionally, SMA is desirable for its pseudoelastic behavior above the material-specific austenite finish temperature ( $A_f$ ). This material property enables a SMA to utilize the stress-induced transformation (as opposed to temperature-induced transformation that characterizes the shape memory effect) and return to shape as the applied loads are relieved.<sup>7,9</sup>

SMA knitted actuators are composed of SMA wire configured into traditional weft knit fabric structures.<sup>10</sup> As shown in Figure 1, weft knits are composed of a series of interlaced loops that form a structurally compliant fabric organized in repeated wales (columns) and courses (rows). Upon thermal actuation, the imposed bending deformation of each knitted loop attempts to return to a remembered straight configuration, forcing a broadening and shortening of macroscopic dimensions. Prior characterization has found contractile SMA knitted actuators (i.e. garter and jersey knit structures) are capable of actuation contraction between 4-40% and generated forces between 2-14 N due to the shape memory effect.<sup>2,11</sup> Both actuation contraction and generated forces are tunable with changes in SMA wire diameter ( $d$ ) and knit index ( $i_k$ ), a non-dimensional value similar to the spring index that quantifies knit density.<sup>11</sup> Additionally, prior work has found that SMA knitted actuator forces increase linearly when scaled in parallel (i.e. increase the number of wales) and actuator actuation displacement increases linearly when scaled in series (i.e. increase the number of courses).<sup>12</sup> This prior research determined that 10 wales by 10 courses is the minimum critical number required to observe scalable behavior; consequently, 10 courses is the minimum critical number by which increasing wales produce increasing forces.<sup>12</sup>

## B. Active-Contracting Orthostatic Intolerance Garment (OIG)

This research specifically evaluates SMA knitted actuators for use in orthostatic intolerance garments (OIG). OIG are medical-grade, lower body compression garments worn by astronauts during reentry, landing, and egress. Historically, these garments have been designed with pneumatic bladders and/or cinching mechanisms (e.g. lacing, straps) to generate on-body pressure through increased wall tension.<sup>13</sup> Other OIG use elastane fabrics in an undersized garment pattern to increase wall tension upon donning.<sup>13</sup> While elastane fabrics and cinching mechanisms offer simple methods to achieve on-body pressure, pneumatic systems have been preferred for their dynamic capabilities. To reduce the mobility concerns of inflated garments,<sup>14</sup> actuators that enable low-profile, untethered, and dynamic compression are considered.

SMA knitted actuators are promising structures for aerospace garment applications due to their surface-wide distributed forces and deformation potential. Prior work has characterized the medical compression capabilities of SMA knitted actuators for low-body use could exceed 65 mmHg (8.7 kPa). Total compression on the body is dependent on a number of variables, including (1) geometric design parameters,<sup>11</sup> (2) macroscopic engineering strain,<sup>2</sup> and (3) anthropometry. Larger diameter SMA wires contain more active material, which

produce higher forces than smaller diameter wires containing less total SMA material. Additionally, straining SMA knitted actuators increases both the generated and total force by leveraging the hysteretic material behavior. Consequently, a garment that begins moderately fitted around the body will exhibit a larger force increase than a garment that begins loose on the body.<sup>2</sup> Finally, body cross-sectional dimensions determine the overall pressure that will be experienced at any anatomical location.<sup>15</sup> Specifically, cross-sections with a smaller radii (e.g. ankle) will experience more pressure than cross-sections with a larger radii (e.g. waist) with the same SMA knitted actuator forces.<sup>2</sup> In addition to cross-sectional dimension, on-body compression is affected by underlying tissue density, topographical variability, dimensional change due to posture, and dimensional change due to fluid shifts in response to changing gravitational conditions.<sup>16</sup> Figure 1 suggests how SMA knitted actuators may be integrated into an aerospace compression system in future work.

### C. Shape Memory Alloy (SMA) Materials

The temperatures that trigger a shape memory response from SMA, specifically the martensite start ( $M_s$ ), martensite finish ( $M_f$ ), austenite start ( $A_s$ ), austenite finish ( $A_f$ ), are dependent on alloy chemistry, specifically the ratio of nickel (Ni) to titanium (Ti), thermomechanical processing, and the presence of additives, such as hydrogen, carbon, oxygen, and nitrogen.<sup>7</sup> NiTi is generally equiatomic, containing 50% nickel and 50% titanium.<sup>17</sup> Higher percentages of nickel produce SMA with a lower austenite finish temperature ( $A_f$ ).<sup>17</sup> Heat-treatment is a method that forces nickel precipitation and is often used to increase the austenite finish temperature ( $A_f$ ) post-fabrication.<sup>18</sup> In the heat-treatment processes, the temperature applied (e.g. 450-550°C), duration of exposure (e.g. 0-25 min.), and quenching methods are all factors that affect the end behavior of the heat-treated specimen.<sup>18</sup> Prior research demonstrates that heat-treatment is an effective method to increase the austenite finish temperature ( $A_f$ ); however, this method does not enable lowering the austenite finish temperature ( $A_f$ ) or fine tuning of other transitions temperatures, such as austenite start ( $A_s$ ), martensite start ( $M_s$ ), and martensite finish temperatures ( $M_f$ ).<sup>18,19</sup>

The most commonly-used commercially available SMA wire is Flexinol® actuator wire by Dynalloy, Inc., which is available with an actuation finish temperature ( $A_f$ ) of approximately 70°C or 90°C. Fort Wayne Metals offers actuator wire with actuation finish temperatures ( $A_f$ ) of -15°C, 0°C, 18°C, 22°C, 40°C, 80°C, or 85°C;<sup>20</sup> however, these materials must be ordered in large quantities (e.g. 1067 meters), making them less commonly used for research prototyping. Nitinol #8 has an austenite start temperature ( $A_s$ ) of 10-35°C and an austenite finish temperature ( $A_f$ ) of 22-40°C, designed specifically for applications that require shape memory phase transition at body temperature.<sup>20</sup> While Nitinol #8 is an excellent option for actuation at body core temperature ( $T_{core} = 37°C$ ), actuation at skin surface temperature is difficult to control due to the low austenite start temperature ( $A_s = 10-35°C$ ) and the wide range of the austenite finish temperatures ( $A_f = 22-40°C$ ).<sup>6,19</sup> Efforts have been made to prevent actuation of Nitinol #8 in ambient environmental temperatures ( $T_{amb} \approx 25°C$ ) before the material touches the body ( $T_s \approx 31°C$ ) through additional heat-treatment;<sup>19</sup> however, this procedure does not narrow the window between the austenite start ( $A_s$ ) and austenite finish temperatures ( $A_f$ ) and uniformly pushes the wide band of actuation

temperature to higher temperatures. A wide temperature range between austenite start and finish temperatures ( $A_s \rightarrow A_f$ ) is not ideal from a power perspective because it means more heat is required to fully actuate the system.

This research presents an alternative strategy to enable on-body actuation and reduce system power requirements. We present a nickel-rich SMA designed by Fort Wayne Metals (i.e. a modification of NiTi #4) for actuation control on the surface of the human skin. Unlike Nitinol #8, which has a wide band of actuation of up to 30°C (i.e. 10-40°C), this custom material (NiTi #4) was designed with a narrow actuation band of 6°C (i.e. 34-41°C) to reduce the power required to fully actuate the system. In addition to the narrow actuation band ( $A_s \rightarrow A_f$ ) and low operating temperatures, which reduces the system power requirements, the SMA material is designed to remain fully actuated upon cooling down to skin temperature, as shown in Figure 2. Within an actuator structure, we found that the SMA material not only maintains maximum forces for a portion of cool down, but actually increases and reaches peak forces upon cool down. Unlike prior work that required high temperatures (e.g. 70°C, 90°C) and continuous heat to power a system, the implication of this strategy is a system that requires a fraction of the heat (e.g. 41°C) to initiate actuation and remains fully stiffened upon equilibrating with skin temperature ( $T_S \approx 31^\circ\text{C}$ ), thus consuming less power and generating less waste heat than a system that needs to be sustained at high temperatures. This novel control strategy provides a new perspective on the power and control assumptions of SMA actuated systems, opening new doors for low-power, actuating wearables.

## II. Experimental Procedures

To observe the force / temperature behavior of the actuator architectures, both the material elements (i.e. SMA wires) and the structural configurations (SMA knitted actuators) were characterized. Two SMA materials were characterized, including Dynalloy wire (70°C Flexinol®,  $d = 0.005''$ ,  $A_f = 61^\circ\text{C}$ ) and Fort Wayne Metals wire ( $d = 0.0056''$ ,  $A_f = 41^\circ\text{C}$ ). The stated transition temperatures for both Dynalloy and Fort Wayne Metals materials are outlined in Table 1. In addition to straight wire testing, both materials were used to fabricate SMA knitted actuators, specifically identical jersey knit structures composed of 15 courses by 15 wale knit loops with knit indices of 124  $\text{mm}^2/\text{mm}^2$ . The SMA knitted actuators were fabricated using a manual weft knitting machine (Taitexma TH-860). Specifications for SMA knitted actuator samples are outlined in Table I.

Experimental characterization was conducted with a standard tensile testing machine equipped with a thermal chamber, a 25-lb load cell, and pneumatic side action grips pressurized to 50-60 psi (Instron model #3365). While the pneumatic grips were sufficient to grip SMA wire (Figure 3, left), SMA knitted actuators samples required a coupling to apply even tensile force to the sample. The custom coupling was fabricated from an aluminum u-channel, t-bar, and threaded connecting rod, depicted in Figure 3, right. Split rings, which began and ended each knitted loop, were threaded along the horizontal connecting rod of the coupling, which was clamped in place by the pneumatic grips. The testing setup used to obtain experimental data for each sample specimen is depicted in Figure 3.

Each wire and actuator sample was characterized through a custom displacement-control characterization designed to evaluate the feasibility of the proposed reduced-power control strategy. The standard displacement-control characterization is a common test performed on SMA actuators to quantify actuator pull force when constrained to a given stretched length.<sup>12,22</sup> By controlling the length of the sample and exposing the sample to repeated thermal loading and unloading, the displacement-control test enables observation of repeatable forces above the austenite finish temperature and below the martensite finish temperature at a fixed displacement. The characterization method is useful for compression garment applications because it mimics the behavior of a material wrapped around the body and actuated when fit snugly or loosely in relation to the body. The test method, which is designed to observe performance repeatability, assumes a uniform actuator pull force. Sources of error could include load cell calibration ( $\pm 0.05\%$  accuracy, 25-lb load cell) or thermal drift as well as displacement transducer calibration ( $\pm 0.05\%$  of frame displacement range). A full description of the standard displacement-control characterization method is detailed in prior work.<sup>2,12</sup>

The custom displacement-control test was designed to include force measurement at approximate skin temperature ( $F_S$ ) in addition to force measurement above the austenite finish temperature ( $F_A$ ) and forces below the martensite finish temperature ( $F_M$ ). As shown in Figure 3, the sample, locked at an approximate martensite free length, specifically martensite length under zero load ( $F \approx 0.02$  N,  $T \approx 25^\circ\text{C}$ ), was heated above the austenite finish temperature ( $A_f$ ) over approximately 5 minutes. The sample then soaked above the austenite finish temperature ( $A_f$ ) for 10 minutes. At the end of the austenite soak, force was recorded ( $F_A$ ), shown at point 1 in Figure 4. The temperature was then decreased to approximately skin temperature ( $T_S$ ), followed by a 30-minute soaking period. The force at approximate skin temperature ( $F_S$ ) was recorded at the end of the second soak, shown at point 2 in Figure 4. Finally, the temperature was decreased below the martensite finish temperature ( $M_f$ ) and the sample soaked for 5 minutes. The force below the martensite finish temperature ( $F_M$ ) was recorded at the end of the third soak, shown at point 3 in Figure 4. The thermal cycle depicted in Figure 4 was repeated three times to observe repeatability. At the end of the third thermal cycle, the sample was slowly displaced (2 mm/min) to a new stretched length. SMA wire samples began at an initial length of 101.6 mm and were displaced in 2 mm increments with a total end length of 107.6 mm. SMA knit actuator samples began at an initial length of 31.5 mm and were displaced in 5 mm increments with a total end length of 61.5 mm.

To account for the transformation temperature difference between the Fort Wayne Metals material and the Dynalloy material (see Table I), the thermal cycle applied to the Fort Wayne Metals samples differed from those applied to the Dynalloy samples. See Figure 4. The Fort Wayne Metals samples were cycled between  $70^\circ\text{C}$ ,  $31^\circ\text{C}$ , and  $-60^\circ\text{C}$ , which were above the material-specific austenite finish temperature ( $A_f$ ), at approximate skin temperature, and below the martensite finish temperature ( $M_f$ ), respectively. Alternatively, the Dynalloy samples cycled between  $90^\circ\text{C}$ ,  $59^\circ\text{C}$ , and  $20^\circ\text{C}$ , which were above the material-specific austenite finish temperature ( $A_f$ ), at pseudo-skin temperature, and below the martensite finish temperature ( $M_f$ ), respectively. The pseudo-skin temperature ( $T_{PS} = 59^\circ\text{C}$ ) was used in place of an approximate skin temperature ( $T_S = 31^\circ\text{C}$ ) because the transition temperature of

the Dynalloy material is not optimized for skin-surface control and a temperature below 33°C would transform the sample to a martensitic state. To compare the behavior of Dynalloy wire and actuator samples to Fort Wayne Metals wire and actuator samples, the pseudo-skin temperature ( $T_{PS}$ ), which is a scaled temperature representative of a drop in temperature, was calculated as a percentage along the cool-down path. Approximate skin temperature ( $T_S \approx 31^\circ\text{C}$ ) is 11.2% below the Fort Wayne Metals austenite finish temperature ( $A_f = 41^\circ\text{C}$ ) and 88.8% above the martensite start temperature ( $M_s = -48^\circ\text{C}$ ). Likewise, the pseudo-skin temperature selected for comparison ( $T_{PS} = 59^\circ\text{C}$ ) is 11.2% below Dynalloy's austenite finish temperature ( $A_f = 61^\circ\text{C}$ ) and 88.8% above the martensite finish temperature ( $M_s = 45^\circ\text{C}$ ). Thermal cycling used in the experimental procedures in depicted is Figure 4.

### III. Results

To evaluate the observed structural response of an actuator architecture, the individual elements used to construct the actuator require parallel investigation. Consequently, the material responses and the actuator structural deformation responses were characterized separately to gain a first glimpse at the nature of the material/structural coupling for these architectures. The results are representative of single sample cycled three times through the thermal cycles depicted in Figure 4 to observe repeatability. Table II presents the mean observed austenite force ( $F_A$ ), martensite force ( $F_M$ ) and force at skin, or pseudo-skin temperature ( $F_S$ ,  $F_{PS}$ ) from three repeated trials. These values are paired with their calculated standard deviation. The result plots below represent the second thermal cycle per tested length ( $L_{1,2,3,\dots,n}$ ) for representation and clarity.

#### A. SMA Wire Characterization

The force-temperature behavior observed during custom displacement-control testing of Fort Wayne Metals NiTi #4 wire and Dynalloy 70°C Flexinol® wire is presented in Figure 5. Figure 5 also isolates the thermal loading and unloading path of both materials at 2% engineering strain to highlight their performance differences. Fort Wayne Metals wire exhibited lower forces than Dynalloy Flexinol® wire at equivalent strain percent. In addition to the magnitude of generated force, the force paths of thermal loading and unloading are noticeably different. Dynalloy Flexinol® wire exhibited a clockwise hysteresis path, generating higher forces upon thermal loading and lower forces upon thermal unloading. Alternatively, at 0% strain Dynalloy Flexinol® took a circuitous path, traversing lower forces between 90-59°C upon thermal loading and higher forces upon thermal unloading. Fort Wayne Metals wire exhibited a circuitous, counterclockwise hysteresis path upon thermal loading and unloading. At moderate strains (e.g. 2%-4% strain), Fort Wayne Metals wire exhibited maximum generated force, or the force differential between austenite and martensite states. Dynalloy Flexinol® exhibited the largest generated forces at lower stretched lengths (e.g. 0%).

#### B. SMA Knitted Actuator Characterization

The results of the SMA knitted actuator characterization are depicted in Figure 6. Plots presented at the top of Figure 6 display the results in full while the plots presented at the bottom of Figure 6 display a close-up of results under 6 N of force. For each stretched

length, both Fort Wayne Metals and Dynalloy Flexinol® actuators exhibited an increase in force from martensite (low temperature) to austenite (high temperature) states until hitting large, macroscopic stretched lengths, findings consistent with prior work.<sup>2</sup> Additionally, the results show that both actuators generally increase generated forces at higher stretched lengths as observed in prior investigations.<sup>2</sup> While the thermomechanical loading and unloading paths were different for Fort Wayne Metals and Dynalloy Flexinol® straight wire, the thermomechanical loading and unloading paths for both actuators constructed from two different materials are visually equivalent. Both SMA knitted actuators exhibit circuitous, counterclockwise hysteresis behavior that forms a figure eight just above the material-specific austenite finish temperature. This thermomechanical behavior becomes more pronounced at moderately stretched lengths (e.g. 32-48%) and flattens out as increased structural strain inhibits intrastructural mobility. Both actuators also exhibit a characteristic parabolic cool-down path that peaks and maintains that peak for the 30-minute hold around approximate skin and pseudo skin temperature ( $T_S = 31^\circ\text{C}$ ,  $T_{PS} = 59^\circ\text{C}$ ) at moderately stretched lengths (e.g. 32-48%).

#### IV. Discussion

The results of the SMA wire and SMA knitted actuator characterization require additional testing beyond the scope of this manuscript to fully identify the variables that induce the observed behavior, spanning SMA manufacturing, training, actuator manufacturing, and testing methodology; however, the observed behavior is discussed through the lens of existing research to enable a specific discussion of the implications for compression garment design.

##### A. SMA Wire Characterization

The thermomechanical response of SMA actuator wire is largely dependent on the processing procedures of the material.<sup>23</sup> Nickel-rich SMA actuator wire (Fort Wayne Metals material) is heavily cold-worked to induce consistent actuator performance, while properties obtained in titanium-rich SMA (Dynalloy Flexinol®) actuator wire are largely obtained through thermomechanically cycling the material (otherwise known as ‘training’). During ‘training’, SMA is thermomechanically cycled such that martensite lattices are gradually re-oriented to preference a particular orientation favorable to linear loading and unloading. Consequently, during displacement-controlled procedures when actuation contraction is prohibited, the trained orientation of the martensite variants produce higher forces than the austenite state at higher strain percent. Alternatively, cold-working is the process of gradually reducing SMA wire diameter through repeated mechanical drawing. Cold-working induces dislocations within the micro structure, resulting in higher strains required to detwin martensite variants to observe the shape memory effect.<sup>23</sup>

Nickel-rich SMA (e.g. Fort Wayne Metals material) generally exhibits weaker forces than titanium-rich SMA (e.g. Dynalloy Flexinol® material) due to difference in material strengths and thermomechanical training; consequently, it is expected that Dynalloy Flexinol wire would reach higher forces than Fort Wayne Metals wire per equivalent strain. Additionally, it is possible that the engineering strains between the samples were not



perfectly equivalent due to the experimental design. Both SMA wires were placed between the side action pneumatic grips at ambient room temperature with an initial displacement of 101.6 mm. While the transition temperature outlined in Table I show that Dynalloy Flexinol® wire should be completely martensitic at ambient room temperature ( $T_{amb} \approx 25^{\circ}\text{C}$ ), Fort Wayne Metals wire may have been partially austenitic from handling, depending on fingertip temperature upon fixture loading. Without knowing the exact material state of the test specimen upon loading into the testing fixtures, it is difficult to determine the exact comparability of the engineered strains.

While more research is required to fully explain the displacement-controlled behavior of both Fort Wayne Metals and Dynalloy Flexinol® wire, the results of this work show that Fort Wayne Metals NiTi #4 wire and Dynalloy 70°C Flexinol® wire are two very different materials that one would expect to exhibit different thermomechanical behavior in a particular system design, such as compression garments.

## B. SMA Knitted Actuator Characterization

While the SMA wire characterization shows that Fort Wayne Metals wire and Dynalloy Flexinol® wire are inherently different materials with different thermomechanical properties, the SMA knitted actuator characterization shows that the structure overrides the wire performance. Consequently, the results of the SMA knitted actuator characterization show that it is possible to leverage the low-temperature benefits of a nickel-rich SMA and still reach the forces achievable with a titanium-rich SMA through structural actuator design. Although additional experimental research is required to explore the variables of the SMA knitted actuators and testing methodology, the thermomechanical behavior was repeatable and suggest an intriguing behavior that could be leveraged for a reduced-power systems actuation control strategy.

Further characterization work is required to detail the thermomechanical behavior that enables a force increase upon cool down. One possibility is that the bending-dominant jersey knit structure experiences highly localized and variable strain, causing different parts of the wire to transition between different thermomechanical paths. As shown in the SMA wire displacement-controlled tests, higher levels of material strain can produce a higher force martensite state and a lower force austenite state (see 6% strain data in Figure 5). Additionally, martensite variants that occur under compression, as partially present under bending deformations, can produce stiffer martensitic behavior than the austenitic or tensioned martensitic variants.<sup>24</sup> Consequently, the knitted loop connection points may be stiffening upon cool down as those high-load bearing points transition from austenite (lower force) to martensite (higher force). Because the level of material strain throughout the individual elements making up the actuator is varied, the total generated pull forces may eventually drop as other, lower-strain areas of the knit structure revert from austenite (higher force) to martensite (lower force) (see 2% strain data in Figure 5).

Given the findings, the results suggest that SMA systems are not limited to power-hungry control strategies, as have been previously demonstrated.<sup>1,2</sup> Rather than continuous heating well beyond temperatures that can be tolerated proximal to human skin (e.g. 70°C, 90°C), the results show that SMA materials designed with lower austenite finish temperatures ( $A_f$ )

(e.g. 41°C) exhibit similar mechanical responses in SMA knitted actuator configurations. Additionally, the results show that structural design can override the force difference of individual materials (i.e. Dynalloy 70°C Flexinol® and Fort Wayne Metals NiTi #4), specifically when the performance of the structure is dependent on a change in material stiffness. Finally, the results present an intriguing phenomenon – that structural design can cause an actuator not just to maintain peak actuation forces upon cool down, but rather increase in force upon cool down. While on-body pressure is partially determined by the relation between garment-body dimensions as well as by SMA knitted actuator geometric design parameters (i.e. wire diameter ( $d$ ) and knit index ( $i_k$ )), future work will characterize the degree of force/pressure control through different applied thermal loads. This behavior has major implications for power and control strategies for wearable aerospace systems as well as for wearable and non-wearable soft robotic systems. The results of this research present a path forward for active-contracting orthostatic intolerance garments as well as for other future actuating systems.

## V. Conclusion

Wearable aerospace systems, such as orthostatic intolerance garments, have traditionally applied pressure to the body through pneumatic actuation.<sup>25</sup> Because these aerospace garments must operate in environments with both limited resources and cargo space, non-pneumatic alternatives include completely passive, adjustable systems, such as undersized elastane garments.<sup>26</sup> These passive systems are limited in their ability to respond to both environmental or anthropometric changes during spaceflight, including increasing gravitational stress upon reentry or gradual limb volume loss.<sup>27,28</sup> While energy-dense, smart materials, such as SMA, have been proposed for use in dynamic aerospace systems, prior investigations have demonstrated on-body force capabilities with materials with large energy demands.<sup>1,2</sup> This manuscript presents an alternative control strategy for wearable, SMA-powered aerospace systems with a fraction of the power requirements of prior demonstrations. A new, nickel-rich SMA material is presented, designed with both low actuation temperature requirements ( $A_f = 41^\circ\text{C}$ ) and a narrow actuation window (i.e.  $6^\circ\text{C}$ ) to reduce the quantity of heat required to initiate full actuation. Additionally, an actuation structure is presented that overrides the material-specific performance differences between nickel-rich and titanium-rich SMA materials. These SMA knitted actuator structures were also found to increase forces upon cool down. Consequently, the proposed control strategy is one that requires momentary heating just over skin temperature and reaches maximum forces upon equilibrating with skin temperature.

This technology shows great promise for use in dynamic OIG during reentry, landing, and egress. The basis for this recommendation is one of functional promise - the materials demonstrate repeatable actuation capabilities sufficient to generate counter-pressures needed for OIG use; however, ultimate adoption of this technology for OIG use requires both functional and operational consideration. Additional analysis of the implications of their operational use (e.g., IVA environment compatibility, off gassing, and flammability considerations) is warranted. Additional systems operation considerations include heating/cooling time and the effects of increased metabolic load and skin temperature during the

landing sequence. This new control strategy offers new opportunities for dynamic aerospace systems and opens a new way of thinking about how these dynamic systems are powered.

## Acknowledgments

This work was supported by a NASA Space Technology Research Fellowship (grant #80NSSC17K0158). Thank you to the Wearable Technology Lab and MnDRIVE for enabling this research through the use of the Instron equipment. A special thank you to Heidi Woelfle for coordinating numerous liquid nitrogen orders. The authors would also like to acknowledge the support of Shawn Chaney, Jack David, and Jeremy Schaffer from Fort Wayne Metals for manufacturing and supplying the experimental materials. Additionally, thank you to Charles Weinberg for designing the Instron coupling.

## Nomenclature

$A_f$	austenite finish temperature
$A_s$	austenite start temperature
$d$	wire diameter
$F_A$	force above the austenite finish temperature
$F_M$	force below the martensite finish temperature
$F_{PS}$	force at pseudo-skin temperature
$F_S$	force at skin temperature
$i_k$	knit index
$M_f$	martensite finish temperature
$M_s$	martensite start temperature
<b>OIG</b>	orthostatic intolerance garment
<b>SMA</b>	shape memory alloy
$T_A$	temperature above austenite finish temperature
$T_{amb}$	ambient temperature
$T_{core}$	core body temperature
$T_M$	temperature below martensite finish temperature
$T_{PS}$	pseudo-skin temperature
$T_S$	skin temperature

## References

1. Holschuh BT, Newman DJ. Morphing Compression Garments for Space Medicine and Extravehicular Activity Using Active Materials. *Aerosp Med Hum Perform.* 2016;87(2):84–92. doi:10.3357/AMHP.4349.2016. [PubMed: 26802372]

2. Granberry RM, Eschen KP, Abel JM, Holschuh BT. Medical Capability of Dynamic Countermeasure Garment for Post-Spaceflight Orthostatic Intolerance. (*under Rev.* 2019).
3. Buckner TL, Kramer-Bottiglio R. Functional fibers for robotic fabrics. *Multifunct Mater.* 2018;1(1):012001. doi:10.1088/2399-7532/aad378.
4. Duvall J, Granberry R, Johnson C, et al. The Design and Development of Active Compression Garments for Orthostatic Intolerance. *ASME J Med Devices.* 2017.
5. Pettys-baker R, Schleif N, Lee JW, et al. Tension-Controlled Active Compression Garment for Treatment of Orthostatic Intolerance. In: *Proceedings of the 2018 Design of Medical Devices Conference.* ; 2018.
6. Granberry R, Ciavarella N, Pettys-Baker R, Berglund ME, Holschuh B. No-Power-Required, Touch-Activated Compression Garments for the Treatment of POTS. In: *Proceedings of the 2018 Design of Medical Devices Conference.* Minneapolis: ASME; 2018.
7. Rao A, Srinivasa AR, Reddy JN. Design of Shape Memory Alloy (SMA) Actuators.; 2015. doi:10.1007/978-3-319-03188-0.
8. Lagoudas DC, ed. *Shape Memory Alloys: Modeling and Engineering Applications.* New York: Springer Science+Business Media, LLC; 2008. doi:10.1007/978-0-387-47685-8.
9. NASA Glenn Research Center. Reinventing the Wheel, <https://www.nasa.gov/specials/wheels/>. Published 2017. Accessed January 3, 2019.
10. Abel J, Luntz J, Brei D. Hierarchical architecture of active knits. *Smart Mater Struct.* 2013;22(12):16. doi:10.1088/0964-1726/22/12/125001.
11. Eschen K, Abel J. Performance and prediction of large deformation contractile shape memory alloy knitted actuators. *Smart Mater Struct.* 2019;28(2):25014. <http://stacks.iop.org/0964-1726/28/i=2/a=025014>.
12. Eschen K, Granberry R, Abel J. Guidelines on the Design, Characterization, and Operation of Shape Memory Alloy Knitted Actuators. (*under Rev.* 2019).
13. Ribeiro LC, Lee SMC, Brown AK, Stenger MB, Platts SH. Countermeasures to Space-flight-induced Orthostatic Hypotension. *Hum Heal Med.* 2009:27–29.
14. Lee SMC, Guined JR, Brown AK, Stenger MB, Platts SH. Metabolic consequences of garments worn to protect against post-spaceflight orthostatic intolerance. *Aviat Sp Environ Med.* 2011;82(6):648–653. doi:10.3357/ASEM.3039.2011.
15. Macintyre L Designing pressure garments capable of exerting specific pressures on limbs. *Burns.* 2007;33(5):579–586. doi:10.1016/j.burns.2006.10.004. [PubMed: 17482762]
16. Granberry R, Dunne LE, Holschuh B. Effects of Anthropometric Variability and Dimensional Change Due to Posture on Orthostatic Intolerance Garments. In: *International Conference on Environmental Systems.* Charleston; 2017.
17. Buehler WJ, Gilfrich J V., Wiley RC. Effect of Low-Temperature Phase Changes on the Mechanical Properties of Alloys near Composition TiNi. *J Appl Phys.* 1963;34(5):1475–1477. doi:10.1063/1.1729603.
18. Morgan NB, Broadley M. Taking the art out of smart! - Forming processes and durability issues for the application of NiTi shape memory alloys in medical devices. *Med Device Mater Proc Mater Process Med Devices Conf.* 2003:247–252. doi:10.1361/cp2003mpmd247.
19. Ozbek S, Foo E, Lee JW, Schleif N, Holschuh B. Low-Power, Minimal-Heat Exposure Shape Memory Alloy (SMA) Actuators for On-Body Soft Robotics. (*under Rev.* 2019).
20. Fort Wayne Metals Research Products. Nitinol Wire, <https://www.fwmetals.com/materials/nitinol/wire/>. Published 2019.
21. Choon TW, Salleh AS, Jamian S, Ghazali MI. Phase Transformation Temperatures for Shape Memory Alloy Wire. *World Acad Sci Eng Technol.* 2007;25:304–307.
22. Holschuh B, Obropta E, Newman D. Low Spring Index NiTi Coil Actuators for Use in Active Compression Garments. *IEEE/ASME Trans Mechatronics.* 2015;20(3):1264–1277. doi:10.1109/TMECH.2014.2328519.
23. Miller DA, Lagoudas DC. Influence of cold work and heat treatment on the shape memory effect and plastic strain development of NiTi. *Mater Sci Eng.* 2001;308:161–175.

24. Bucsek AN, Paranjape HM, Stebner AP. Myths and Truths of Nitinol Mechanics: Elasticity and Tension – Compression Asymmetry. *Shape Mem Superelasticity*. 2016;2(3):264–271. doi:10.1007/s40830-016-0074-z.
25. Jenkins DR. *Dressing for Altitude*. Washington D.C.: National Aeronautics and Space Administration; 2012.
26. Stenger MB, Lee SMC, Ribeiro LC, et al. Gradient compression garments protect against orthostatic intolerance during recovery from bed rest. *Eur J Appl Physiol*. 2014;114(3):597–608. doi:10.1007/s00421-013-2787-4. [PubMed: 24337701]
27. Nicogossian AE. *The Apollo-Soyuz Test Project Medical Report*. Washington D.C.; 1977.
28. Kravik SE, Ames Research Center. *Cardiovascular, Renal, Electrolyte, and Hormonal Changes in Man During Gravitational Stress, Weightlessness, and Simulated Weightlessness: Lower Body Positive Pressure Applied by the Antigravity Suit.*; 1989.

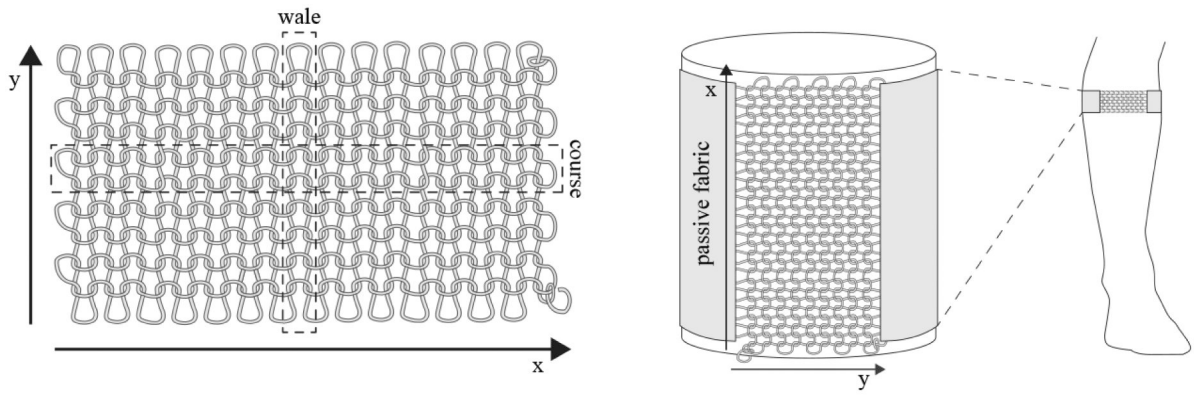


**Figure 1.**

Weft knit fabric structure composed of an interlocking system of loops, forming repeated wales (columns) and courses (rows). Optimal contractive forces are translated to the body when these fabrics are oriented with increasing wales along the length of the body (fabric x-axis) and at minimum 10 courses around the circumference (fabric y-axis). The remaining circumference can be completed with passive fabric.

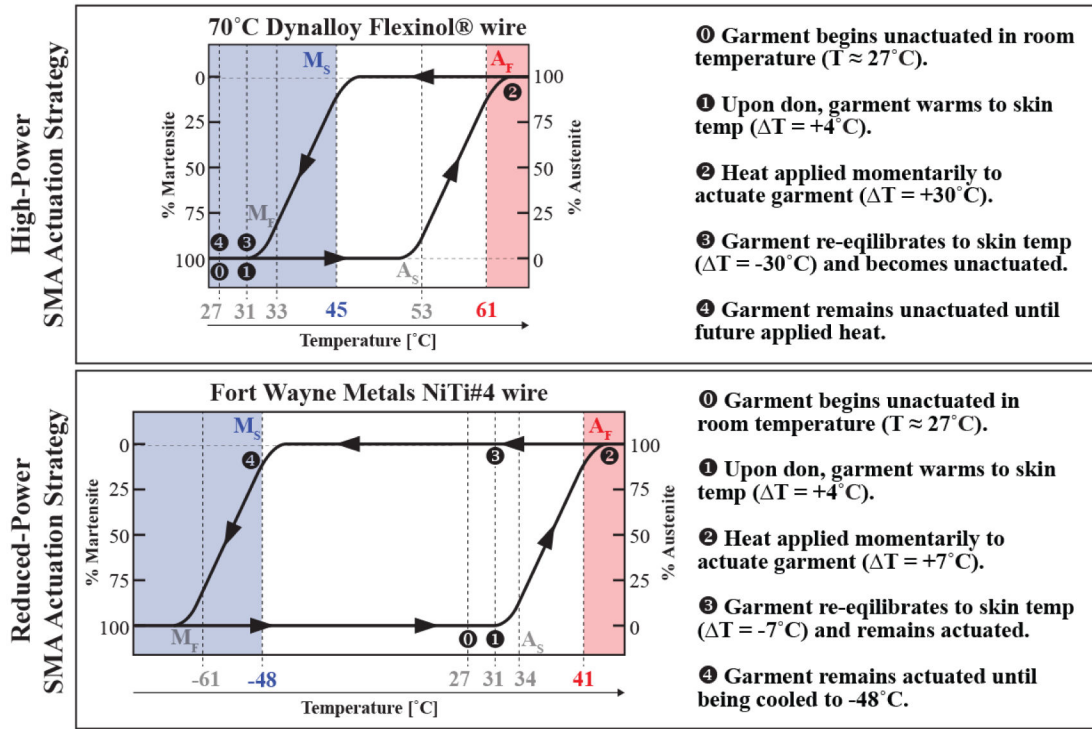


**Figure 2.** Reduced-power SMA actuation strategy in relation to previous high-power SMA actuation strategy.

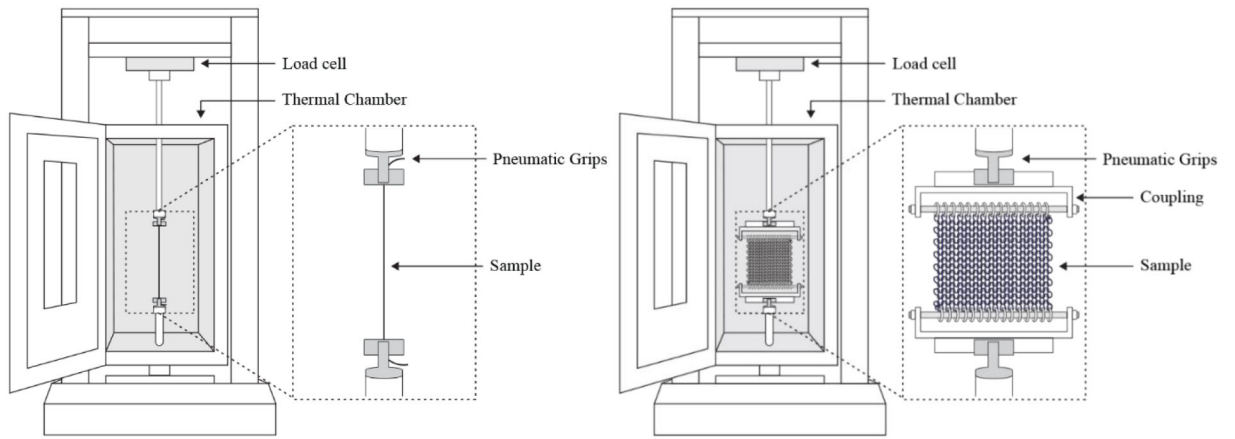


**Figure 3.** Tensile testing equipment (Instron) used to obtain experimental data for each sample specimen. Pneumatic grips were used to grasp straight SMA wire (left). Pneumatic grips and a custom coupling were used to grasp SMA knitted actuators (right)



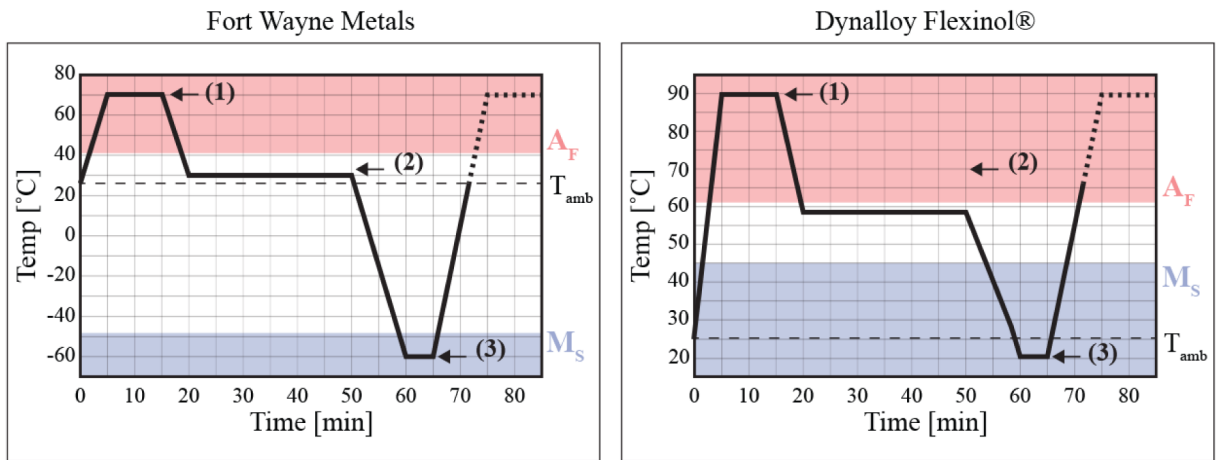


**Figure 4.**

Thermal cycles for custom displacement-control characterization. (1) Force above the austenite finish temperature ( $F_A$ ), (2) Force at approximate skin temperature ( $F_S$ ) or an equivalent temperature drop for the high temperature control material. (3) Force below the martensite finish temperature ( $F_M$ ). Blue depicts martensite-inducing temperatures and red depicts austenite-inducing temperatures.

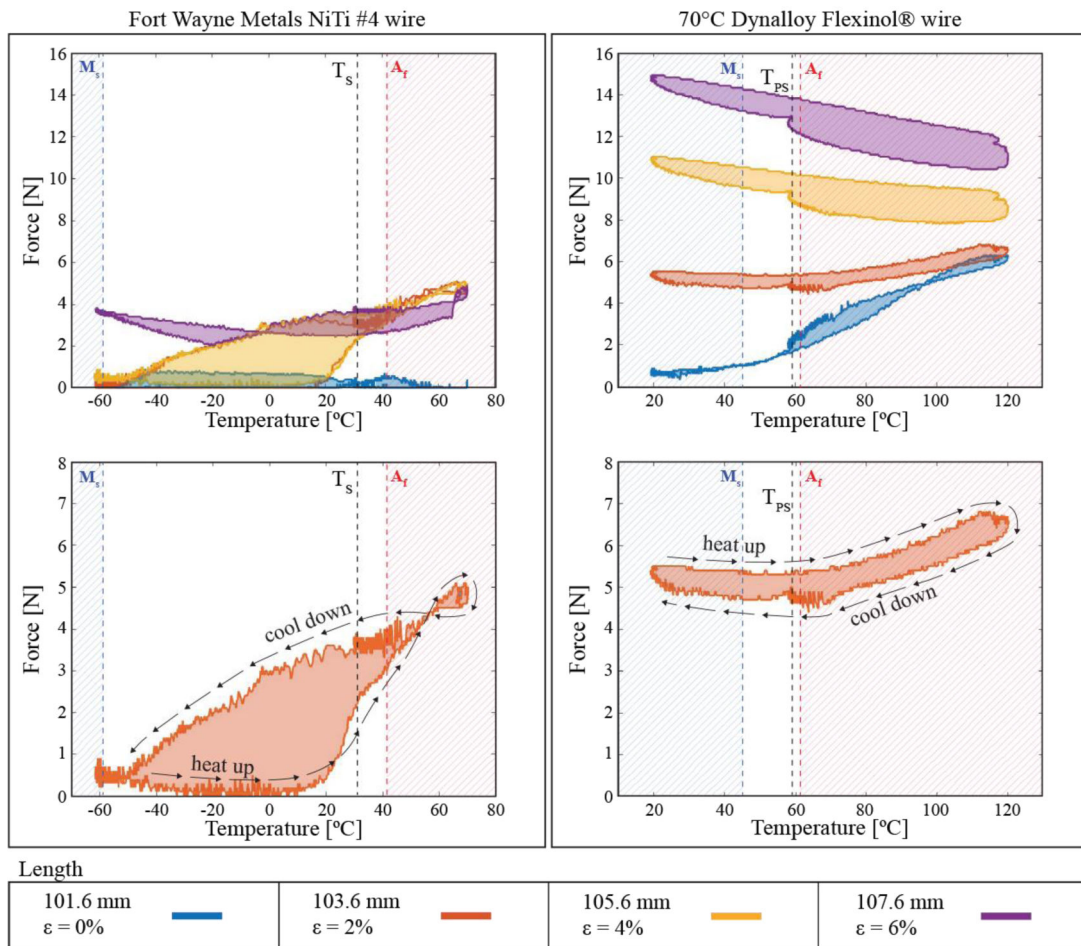


**Figure 5.** Results of custom displacement-control characterization for Fort Wayne Metals and Dynalloy Flexinol® straight wire. Full results are displayed in top plot. Isolated, 2% strain results are displayed in the bottom plots with thermal loading and unloading path directions.

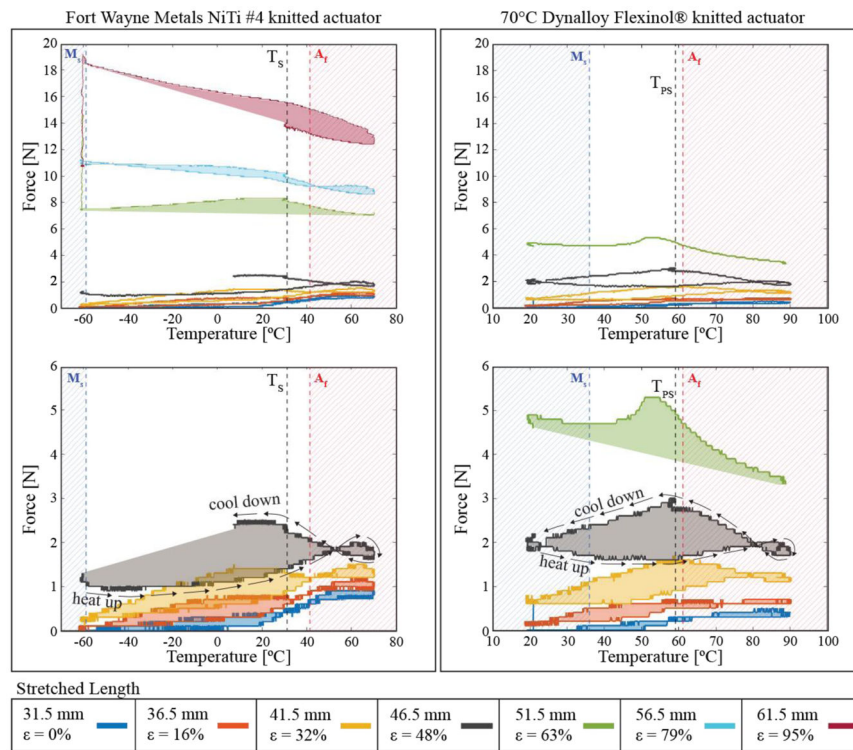


**Figure 6.** Results of custom displacement-control characterization for Fort Wayne Metals and Dynalloy Flexinol® SMA knitted actuator. Full results are displayed in top plot. Results below 6 N of force are displayed in the bottom plots with thermal loading and unloading path directions.

**Table I.**SMA material and actuator specifications.<sup>20,21</sup>

Material	A <sub>f</sub> [°C]	A <sub>s</sub> [°C]	M <sub>s</sub> [°C]	M <sub>f</sub> [°C]	d [in]	i <sub>k</sub> [mm <sup>2</sup> /mm <sup>2</sup> ]	Knit Type
Fort Wayne Metals NiTi #4 <sup>20</sup>	41	34	-48	-61	0.0056	124	Jersey
70°C Dynalloy Flexinol <sup>®21</sup>	61	53	45	33	0.005	124	Jersey

**Table II.**

Statistical results (mean  $\pm$  standard deviation) for NiTi wire and SMA knitted actuators based on three repeated thermal cycles per fixed length ( $L_1, L_2, L_3, \dots, L_n$ ).

		$L_1$	$L_2$	$L_3$	$L_4$	$L_5$
<b>70°C Flexinol Wire</b>	$F_A$ [N]	$6.2 \pm 0.1$	$6.6 \pm 0.1$	$8.4 \pm 0.1$	$10.8 \pm 0.1$	N.A.
	$F_S$ [N]	$1.9 \pm 0.1$	$4.9 \pm 0.1$	$9.5 \pm 0.1$	$13.0 \pm 0.1$	N.A.
	$F_M$ [N]	$0.6 \pm 0.1$	$5.3 \pm 0.1$	$10.9 \pm 0.1$	$14.8 \pm 0.1$	N.A.
<b>NiTi #4 Wire</b>	$F_A$ [N]	$0.0 \pm 0.1$	$4.8 \pm 0.4$	$4.8 \pm 0.3$	$4.6 \pm 0.1^*$	N.A.
	$F_{PS}$ [N]	$0.3 \pm 0.1$	$3.4 \pm 0.1$	$3.8 \pm 0.2$	$3.9 \pm 0.1^*$	N.A.
	$F_M$ [N]	$0.0 \pm 0.0$	$0.1 \pm 0.1$	$0.2 \pm 0.1$	$3.6 \pm 0.1^*$	N.A.
<b>70°C Flexinol Knitted Actuator</b>	$F_A$ [N]	$0.8 \pm 0.1$	$1.0 \pm 0.1$	$1.2 \pm 0.1$	$1.7 \pm 0.1$	$4.2 \pm 1.1^*$
	$F_S$ [N]	$0.5 \pm 0.1$	$0.8 \pm 0.1$	$1.4 \pm 0.1$	$2.5 \pm 0.1^*$	$5.3 \pm 0.8^*$
	$F_M$ [N]	$0.0 \pm 0.0$	$0.1 \pm 0.0$	$0.3 \pm 0.1$	$1.0 \pm 0.1^*$	No data <sup>*</sup>
<b>NiTi #4 Knitted Actuator</b>	$F_A$ [N]	$0.4 \pm 0.1$	$0.6 \pm 0.1$	$1.2 \pm 0.1$	$1.8 \pm 0.1$	$2.6 \pm 0.6^*$
	$F_{PS}$ [N]	$0.3 \pm 0.1$	$0.7 \pm 0.1$	$1.6 \pm 0.1$	$3.0 \pm 0.1$	$4.9 \pm 1.0^*$
	$F_M$ [N]	$0.0 \pm 0.1$	$0.2 \pm 0.1$	$0.6 \pm 0.1$	$1.6 \pm 0.2$	$4.1 \pm 1.1^*$

\* Indicates less than 3 data points used due to equipment errors.